# Anodization of Al(100), Al(111) and Al Alloy 6063 studied *in situ* with X-ray reflectivity and electrochemical impedance spectroscopy

CrossMark

Jonas Evertsson[a],[*], Florian Bertram[b], Lisa Rullik[a], Gary Harlow[a], Edvin Lundgren[a]

[a] *Division of Synchrotron Radiation Research, Lund University, Box 118, 221 00 Lund, Sweden*
[b] *DESY Photon Science, Notkestr. 85, D-22607 Hamburg, Germany*

## ARTICLE INFO

## ABSTRACT

We present results from the anodization of single crystal Al(100) and Al(111) surfaces and the aluminum alloy AA 6063 studied *in situ* by X-ray reflectivity and electrochemical impedance spectroscopy. We observe that the anodic oxide layer grows linearly with the anodization potential and that the thicknesses are similar for all samples. However, the thicknesses obtained from X-ray reflectivity are higher than that obtained from electrochemical impedance spectroscopy. We attribute the higher thicknesses to an outer porous oxide layer, which is not detected by electrochemical impedance spectroscopy. Both, electrochemical impedance spectroscopy and X-ray reflectivity suggests that a more heterogeneous and rough oxide is formed on AA 6063 due to the influence of the alloying elements and intermetallic particles during the growth.

## 1. Introduction

Aluminum and its alloys are used in many everyday applications such as in automobile manufacturing, aerospace and construction. Anodic aluminum oxides are also of interest in future nanotechnology applications [1]. One of the most important properties of aluminum is the natural high resistance to corrosion due to the passivating aluminum oxide film. In ambient conditions an amorphous native oxide film, 2–7 nm thick, is formed on both pure aluminum and industrial aluminum alloys [2–4]. This oxide layer provides good corrosion resistance in many environments and is self-renewing after mechanical damage in ambient and aqueous environments [5]. However, many applications require an even higher level of corrosion protection. A common technique is to grow a thicker oxide by anodic electrochemical anodization. The formed anodic oxide usually consists of a more compact inner barrier oxide layer and a more open outer porous oxide layer [1,6]. Depending on the conditions of anodic growth, where the choice of electrolyte is the most important, the oxide can be almost free from the presence of a porous oxide layer, this is called a barrier-type oxide.

The high importance and attractive properties of aluminum have lead to many studies on aluminum and aluminum oxides over several decades to understand both fundamental and applied aspects. The initial stages of oxidation have been studied both theoretically and with experimental surface science techniques [7–19]. The exact atomic scale structures of crystalline ultrathin and bulk aluminum oxides are known [20–28]. However, less is known about the atomic structure and growth

of aluminum oxides, such as anodic oxides, used for applications due to their complex amorphous structure [29]. For these systems, traditional electron-based methods and techniques based on diffraction fail due to the insulating nature and amorphous structure of the oxides. Furthermore, *in situ* studies with electron based techniques are difficult and technically demanding to perform, due to the short mean free path of the electrons in liquids. Instead, the anodization process and corrosion resistance properties have been extensively studied using for example electrochemical and *ex situ* microscopy techniques. From such studies a large amount of literature exists that aims to improve the anodization processes and create anodic oxides suitable for different technical applications. In this way a number of fundamental processes have successfully been explained. Nevertheless, some aspects are not fully understood and still debated [1,6,30–32].

Aluminum alloys used in applications are polycrystalline materials that in addition to pure aluminum include alloying elements such as Cu, Fe, Mg, Si, and Zn that further complicate studies. These alloying elements are primarily introduced to improve mechanical properties but are also known to influence the anodization process, the resulting anodic oxide and the corrosion resistance of the material [33,34]. Compared to anodic oxides on pure aluminum, the oxides on alloys are more heterogeneous with incorporated particles, voids, cracks, irregular film thickness, roughened surface, and a more disordered metal/oxide interface [33]. The alloying elements are in solid solution where they constitute parts in the more homogenous general alloy material or in intermetallic particles with compositions that are different from the general alloy.

One way to improve the understanding of electrochemical processes such as anodization is to study them under *in situ* conditions. Methods based on hard X-rays, which can penetrate through the electrolyte, combined with suitable traditional chemical methods are therefore suitable for studies in both ambient atmospheric and aqueous conditions [35–40].

In this report, we present the anodization of Al(100), Al(111) and aluminum alloy (AA) 6063 studied *in situ* using combined X-ray reflectivity (XRR) and electrochemical impedance spectroscopy (EIS). We have previously compared separate XRR and EIS measurements using two different electrochemical cells at different locations [35]. In the present article, we take a step forward and perform *in situ* XRR and EIS at the same time. One important goal is to study the possibility of using two interdisciplinary techniques, XRR and EIS, to achieve a better understanding of the structural and electrochemical properties of growing anodic oxides. A second aim is to use the combination of techniques to describe the differences between the anodization of pure aluminum single crystal surfaces and an industrially standard aluminum alloy.

## 2. Experimental

The anodization behavior and anodic oxides on single crystal Al (100) and Al(111) surfaces and an industrial aluminum alloy AA 6063 were investigated. The single crystals with a purity of 99.9999% were purchased from Surface Preparation Laboratory (SPL), Zaandam, The Netherlands. The AA 6063 was cut from an extruded and aged to temper T6 Al profile supplied by Sapa Technology, Finspång, Sweden. The alloying elements in the alloy are 0.20–0.60 wt% Si, 0.35 wt% Fe, 0.10 wt% Cu, 0.10 wt% Mn, 0.45–0.90 wt% Mg, 0.10 wt% Cr, 0.10 wt % Zn and 0.10 wt% Ti [41]. All samples were hat shaped and the top surfaces was polished to a roughness of 0.03 μm or lower by SPL.

The experiments were performed at the PETRA III/DESY beamline P08 [42] in a PEEK cell shown in Fig. 1 and similar to the electrochemical cell described in ref. [43]. Fig. 1 (a) shows an illustration of the cell with the used three-electrode setup. The hat shaped sample (working electrode) is inserted from the bottom, the glassy carbon counter electrode from the top and the miniature Ag/AgCl (eDAQ, Australia) reference electrode from the side with the end positioned in between the counter and working electrode. The cell is sealed using silicone washers and viton o-rings at the positions marked in Fig. 1 (a). The photo in Fig. 1 (b) shows the assembled cell with screws for closing the cell and tubing for the inlet and outlet of the electrolyte. The cylindrical volume with electrolyte is 2–3 ml and have an inner diameter of 8 mm. The cell allows for *in situ* investigation using both XRR and EIS on the same occasion. The electrolyte is possible to easily exchange without moving the cell allowing for continuous experiments without major realignments of the sample to the X-ray beam. A drawback of the



**Fig. 1.** (a) Illustration with a removed section revealing the inside of the PEEK cell used for the combined XRR and electrochemical experiments. A hat shaped sample is the working electrode (WE), a glassy carbon rod the counter electrode (CE) and an Ag/AgCl electrode (RE) the reference electrode. A hard X-ray beam can penetrate the thinner walls of the cell and probe the top of the sample. Viton o-rings and silicone washers are used to seal the cell. (b) Photo of the assembled cell with the attached inlet and outlet tubing.

design is that the side of the sample is in contact with the electrolyte and influence the electrochemical measurements. This means that for Al (100) and Al(111), also non (100) and (111) surfaces influences the electrochemical measurements. However, this is not the case for XRR since the X-ray beam only probes the top of the sample.

The anodization and the EIS were performed with an Autolab PGSTAT204 potentiostat with a FRA32 module using the software Nova 1.9 (Metrohm Autolab B.V. Netherlands). For the EIS a perturbation amplitude of 10 mV and a frequency range from $10^4$ Hz to $10^{-2}$ Hz was used. The EIS data were analyzed using the software Zview (Scribner Associates, USA).

For the XRR measurements a photon energy of 18 keV (0.69 Å) was used and the reflected intensity was measured using a point detector. The XRR measurements were performed by measuring the intensity of a reflected X-ray beam as a function of incidence angle. A complete XRR measurement was obtained in 6–7 min. The XRR curves were analyzed using the software GenX [44]. The software uses the recursive Parrat-algoritm [45] with a Névot-Corce [46] roughness model to simulate the data. In the algorithm, the sample is modelled with layers of different density, thickness and roughness and the reflected intensity is calculated using Fresnel reflectivity of each interface of the multilayer model. The roughness of the interfaces is modelled by a continuously changing electron density connecting the layers and described by an error-function profile.

As the electrolyte, a sodium citrate buffer was used for both the anodization and the EIS. The electrolyte was adjusted to pH 6 by adding sodium hydroxide to a 0.1 M citric acid solution. A neutral buffer solution is typically used to grow more protective barrier-type oxides since the dissolution of the anodic oxide during anodization is minimized [6].

The samples were anodized in an increasing stepwise manner at 2 V, 4 V, 6 V, 8 V and 10 V *vs.* the open circuit potential (OCP) measured before anodization. The OCP was − 0.7 V, − 0.6 V and − 0.8 V for Al (100), Al(111) and AA 6063, respectively. For each step the potential was increased linearly for 100 s until the new potential was reached. After 30 min of anodization at each potential step, XRR and EIS were recorded at the anodization potential.

## 3. Result and discussion

### 3.1. Current transients

During the anodization, the current was measured at each potential. From the current, several characteristics of the growing oxide can be obtained. The current through the oxide film mainly consists of two parts, an electronic and an ionic part, due to the conduction of electrons and ions, respectively [6]. Fig. 2 shows the current response of Al(111) during and after the step from 4 V to 6 V, which also is typical for all potentials and samples studied here. When 6 V is reached, the current exponentially decreases, which indicates the growth of a mainly nonporous compact barrier-type oxide film since the current decreases as a result of a decreasing electric field due to a thicker oxide layer [6]. This characteristic is different to that found for porous-type oxides grown in acidic electrolytes, where the current does not stabilize at a low value. Instead the current increases further and then stabilize at a higher value. This higher current is due to the flow of ions, indicating that the oxide is still growing at this stage [6]. Hence the transients shown indicate the growth of a barrier-type oxide. However, it should be emphasized that the formation of an additional porous oxide layer cannot be excluded since for less acidic electrolytes the typical current transients for porous oxide growth is not as pronounced as for more acidic electrolytes. The reason for the possibility of porous growth in pH neutral electrolytes has been ascribed to a decreasing local pH close to the aluminum surface, which increases the oxide dissolution rate and allows the formation of pores [6,47–50]. The growth rate of the porous oxide is low, due to the weaker ele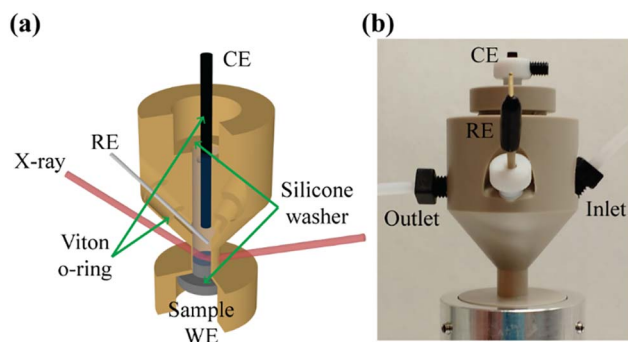ctric field over the relatively thick